

Proceedings of the ISSRNS '94, Jaszowiec 1994

HIGH ENERGY RESOLUTION PHOTOEMISSION BEAM LINE AT ELETTRA

C. QUARESIMA, C. OTTAVIANI, M. MATTEUCCI, C. CROTTI, A. ANTONINI,
M. CAPOZI, S. RINALDI, M. LUCE, P. PERFETTI

Istituto di Struttura della Materia, CNR
Via E. Fermi 38, 00044 Frascati, Italy

K.C. PRINCE, C. ASTALDI, M. ZACCHIGNA, L. ROMANZIN AND A. SAVOIA

Sincrotrone Trieste, Padriciano 99, Trieste, Italy

The storage ring ELETTRA in Trieste, completely dedicated to synchrotron radiation, started its operation in October 1993. We present here the high energy resolution photoemission beam line we have constructed. The beam line has been designed to perform photoemission experiments in the vacuum ultraviolet and soft X-ray. The radiation source is an undulator of type U12.5 and the photon energy range is 18–800 eV. The monochromator is a spherical grating type and the theoretical power resolution is 10^4 in average over the entire energy range. The beam line is now installed and at the time of writing the line is being commissioned.

PACS numbers: 07.65.Eh, 07.85.+n, 79.60.-i

1. Introduction

ELETTRA, the new storage ring of Trieste completely dedicated to synchrotron radiation, has been designed to be one of the brightest synchrotron radiation source in the vacuum ultraviolet (VUV) and soft X-ray region. This is obtained with a large variety of insertion devices such as wigglers and undulators. One of the major benefits of high brightness is the possibility of building a beam line with high spectral resolution and high photon flux. High brightness is due to a very small source area and small angular divergence; these characteristics allow us to use small optical elements, thus reducing the aberration contributions which degrade the energy resolution. The purpose of this paper is to present the main characteristics of the beam line we have constructed in Trieste which is dedicated to photoemission spectroscopy.

High energy resolution is now one of the major demands made by scientists working with synchrotron radiation to the constructors of new third generation

sources. Photoemission with high spectral resolution provide very advanced and detailed information on the chemical status of the elements, and can be used to study chemical processes, in particular those related to surface chemistry, such as passivation, corrosion, catalysis and the fabrication of thin films and interfaces. We can certainly state that there is no scientific subject in the fields of solid state physics, material science, atomic and molecular physics and chemistry, which will not benefit greatly from a high energy resolution photoemission beam line.

2. Beam line layout

Figure 1 shows the beam line layout. The beam line can be divided into three parts: the horizontal M_0 and vertical M_1 focusing mirrors, the monochromator with entrance and exit slits and gratings, the refocusing mirror M_2 . All the focusing optical elements have a spherical shape except the refocusing mirror M_2 which is toroidal.

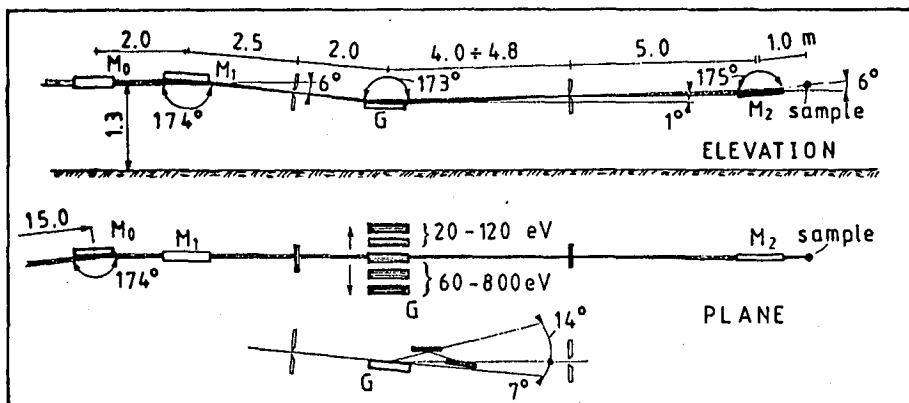


Fig. 1. Beam line layout.

The mirrors M_0 and M_1 , in the Kirkpatrick-Baez mounting [1, 2] focus the source horizontally and vertically on the exit slit and entrance slit, respectively. Both mirrors focus individually in one direction and their optical functions are completely decoupled.

The monochromator is a spherical grating monochromator (SGM) of the type reported in Ref. [3]. Five gratings allow the scanning of an energy range between 18 eV and 800 eV. To cover the energy range 100–800 eV with the required resolution we have chosen a grating deflection angle of 174°, with three gratings covering the high energy range. To maintain good resolution and flux, in the low energy range 18–120 eV, and to avoid the use of gratings with very low line densities, i.e. high limit to the resolution due to diffraction, the deflection angle must be reduced and this is accomplished by a pair of removable plane mirrors as shown in the inset of Fig. 1. The two plane mirrors placed along the output arm leave the monochromator practically unchanged. The remaining two gratings coupled with

the above plane mirrors cover the low energy range 18–120 eV. The beam line was constructed by ISA ITALIA-JOBIN YVON according to our design.

3. The source

The source is an undulator of the type U12.5 [4], where $\lambda_0 = 12.5$ cm is the undulator period. This source was designed to cover the energy range 20–800 eV and some of the characteristics are reported in Tables I, II and III.

TABLE I
Characteristics of the undulator
U12.5 at 2 GeV, 400 mA.

λ_0	12.5 cm
$B_{0\max}$	0.456 T
K_{\max}	5.3
N_{periods}	36 (3 sections)
$P_{\text{tot max}}$	0.95 kW
Tuning range	20–856 eV

TABLE II
Source sizes and divergence computed assuming a total undulator length of 4.5 m, 2 GeV.

Energy	Σ_x [μm]	Σ_y [μm]	$\Sigma_{x'}$ [μrad]	$\Sigma_{y'}$ [μrad]
800	240	45	38	30
200	241	50	57	51
20	253	90	156	154

TABLE III
Power in the central cone (defined as $2\pi\Sigma_x\Sigma_y$), total power and power density as a function of photon energy at 2 GeV photon energy.

Energy	K	P_{tot} [W]	P'_d [W/mrad ²]	P_{cent} [W]	P'_2 [mW/mm ²]
800	1.3	60	27	1.9	32
100	2.0	136	424	13.9	49.3
20	5.3	949	1137	170.4	132

The energy range 20–856 eV can be covered using five harmonics and the maximum photon energy is defined as the energy at which the flux has decreased

to 10% of maximum. The brightness of the undulator is reported in Fig. 2 together with the corresponding curves of a wiggler and of conventional sources like bending magnets. The U12.5 undulator has unique characteristics and produces a brilliance which is several orders of magnitude greater than those obtained with conventional sources of synchrotron radiation.

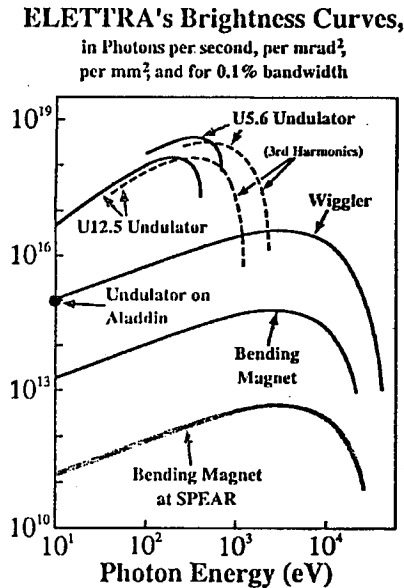


Fig. 2. Brightness of the undulator U12.5 together with the corresponding curves of a wiggler and of conventional sources like bending magnets.

4. The horizontal and vertical focusing mirrors

The horizontal focusing mirror M_0 is spherical and focuses the radiation on the exit slit of the monochromator. It has the additional function of protecting the other optical elements of the beam line from excessive heat and radiation load. The heat load on M_0 can induce figure errors which are not critical to the transmission and resolving power of the monochromator. Taking into account the maximum source divergence and dimension occurring at 20 eV (see Table II), the incidence angle (see Fig. 1) and the distance from the source, which is 15 m, we evaluated an illuminated area of nearly 20 cm \times 1 cm. The actual mirror is made of bulk silicon carbide (SiC) and has dimensions 22 cm \times 5 cm. The mirror is larger than the beam size to allow exposure of different parts of the mirror in case of contamination.

We point out that the use of only planar and spherical shapes for all optical elements, allows the achievement of state-of-the-art in terms of surface smoothness and figure error accuracy. This is because these shapes can be fabricated with greater accuracy than other shapes such as ellipses, toroids, etc. In all our optical

elements, manufactured by Jobin Yvon France, the slope errors and roughness were below 0.5 arcsec and 5 Å.

The vertical focusing mirror M_1 of bulk SiC is also spherical and focuses the radiation on the entrance slit of the monochromator. The demagnification has been chosen so that the light spot at the focus plane does not exceed twice the minimum entrance slit width (10 μm). The size has been evaluated by applying the same criterion used for the previous mirror and it is 22 cm \times 5 cm.

Both mirrors M_0 and M_1 are water cooled through two copper bars in intimate contact with the two long sides of each mirror.

5. The monochromator

The SGM monochromator is composed of entrance and exit slits and of only one optical element between them, the spherical grating. In fact the SGM concept [5] is based on the use of spherical elements for the horizontal and vertical focusing. The SGM monochromator is quite similar to the toroidal grating monochromator (TGM) and the SGM concept was developed to reduce the astigmatism and astigmatic coma produced by the combined effect of the toroidal mirror and toroidal grating in the TGM. In fact the best solution to prevent the horizontal image line from bending would be to use cylindrical optical elements for a complete decoupling of the focusing properties in the horizontal and vertical directions; it was shown [3] that, in the case of low incidence angle, the reduction of the aberrations is preserved using spherical optical elements instead of cylindrical.

The SGM solution has the following characteristic properties [3]:

- It uses spherical elements which can be manufactured more accurately than toroidal or ellipsoidal elements and it is possible to reach extremely good figure errors (the slope error in all our spherical elements is better than 0.5 arcsec).

- The monochromator itself has only three elements and it has an extremely high transmission and high resolving power.

- The horizontal focusing mirror absorbs a large part of the incoming radiation, serving as a heat protector of the following optical elements; in particular the power impinging on the gratings is not critical for the monochromator resolution. Taking from Table III the maximum power density at 20 eV originated from the undulator we can estimate that the power density on a grating, after two reflections on M_0 and M_1 coated with a thin gold film and with a 10 μm entrance slit, is nearly 10 mW/mm². By using simple analytical arguments [6] we estimated that the maximum slope error on the grating induced by the heat load, with the storage ring working at 400 mA and 2 GeV, is 0.3 arcsec, i.e. lower than the figure error obtained by the manufacturer.

- Due to the spherical shape of the optical elements it is possible to select fresh surfaces if radiation damage should reduce the quality of the transmitted beam.

- The decoupled nature of the whole monochromator allows easy alignment and diagnostics of the beam line.

- The scanning mechanism is very simple. The gratings are moved by a sine bar while the exit slit moves linearly to follow the focal position for different

wavelengths. This last movement is not critical and an uncertainty of few centimeters can be tolerated in the position of the exit slit. Three spherical gratings (1400 l/mm, 700 l/mm, 350 l/mm) are provided to cover the soft X-ray range 100–800 eV and two (1600 l/mm, 600 l/mm) for the VUV range 15–120 eV with deflection angles of 174° and 160°, respectively. The grating center is placed 2.5 m far from the entrance slit and 4.0–4.7 m from the exit slit depending on the energy. Every element scans its whole spectral range by a simple rotation of 3°, around its y axis. The accuracy of the grating drive is better than 0.06" and, with a sine bar of 0.5 m long, the accuracy of the linear drive mechanism is 0.15 μm .

The VUV range is covered by two gratings (see inset of Fig. 1) with a deflection angle of 160°. In order to keep the beam line unchanged we inserted a pair of plane mirrors between the gratings and the exit slit. The first mirror is fixed and is located so that it deflects the beam at 7°, of incidence angle. The second mirror is removable and is placed along the output direction to deflect the diffracted beam onto the exit slit.

The ion-etched holographic gratings are made from bulk SiC, are water cooled, and coated with 200 Å Au on top of 40 Å of Cr. The two plane mirrors are pure silica with similar coating materials.

The resolution of the beam line is essentially determined from the two slits and the gratings. The contribution of the slits, with a certain grating dispersion, is determined by their aperture and in our case the maximum resolution can be obtained with 10 μm minimum width. The main limit to the resolution comes

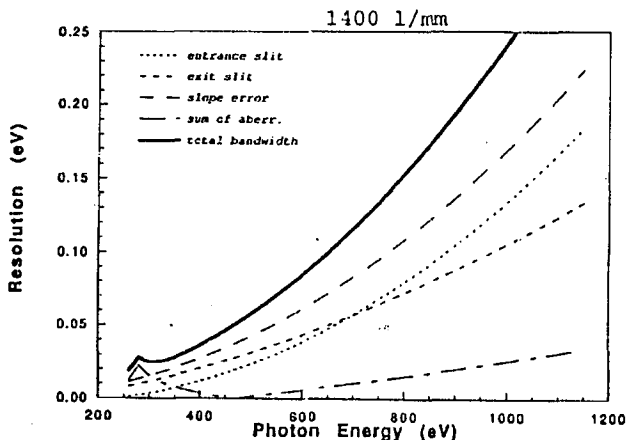


Fig. 3. Resolution limits of the 1400 l/mm grating versus photon energy. The total bandwidth (solid line) is obtained as the root-mean-square (rms) sum of the resolution limits due to: aberrations, 10 μm entrance and exit slits, and to imperfections of the reflecting surface (2.5 μrad rms slope errors). The figure clearly shows that the total bandwidth is mainly limited by slope errors and by minimum slit opening.

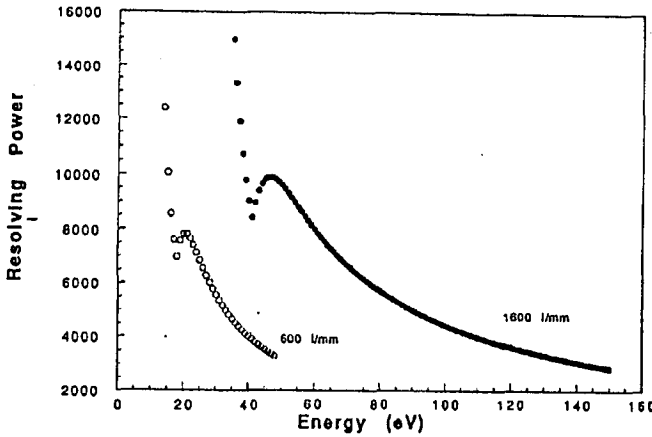


Fig. 4. Resolving power of the low energy gratings in the energy range 15–150 eV. Open circles refer to the 600 l/mm grating; full refer to the 1600 l/mm grating.

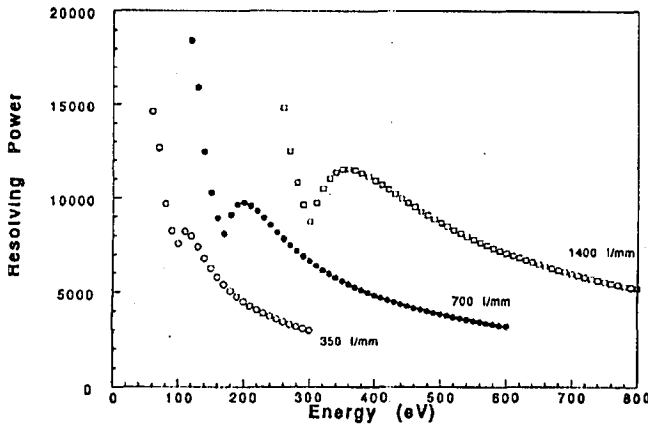


Fig. 5. Resolving power of the high energy gratings in the energy range 60–800 eV. Open circles refer to the 350 l/mm grating; full refer to the 700 l/mm; open squares refer to the 1400 l/mm grating.

from the figure errors due to the grating construction while a minor contribution is due to aberrations. All these contributions can be easily calculated using simple mathematical formulas [3], and the result for the 1400 l/mm grating is reported in Fig. 3 as an example. The calculations for all the gratings are reported in Ref. [7]. From Fig. 3 the critical role played by the slope errors is clear: the present value of 0.5 arcsec contributes more than 50% to the total bandwidth. The resolving power $E/\Delta E$ obtained by the previous calculations [7] for the five gratings is reported in Figs. 4 and 5. These results, which give a theoretical lower limit, show

the incredibly high resolution obtainable with this monochromator; it is always possible to choose a grating to have a resolving power better than 10^4 , except for energies above 500 eV, where $E/\Delta E$ is lower but it never goes below 5000.

6. The refocusing mirror and the experimental chamber

The mirror M_2 (see Fig. 1) is made of pure silica, has a toroidal shape and it has a magnification of 0.2 which leads to an image size on the sample $130 \mu\text{m} \times 12 \mu\text{m}$. Movement of the exit slit can increase a little the minimum spot size on the sample.

The measurement station is equipped for angle-resolved and angle-integrated photoemission as the main experimental methods. The spectrometers, from VSW Ltd., have a theoretical energy resolution of 10 meV in the energy range 20–50 eV and a little worse at higher energies. This means that the resolution of the photons and electrons are well matched except at the very lowest energies. The extraordinary high resolution capability of the beam line can also be exploited by other experimental techniques like absorption or reflection spectroscopy. The chamber is equipped with the usual facilities for surface preparation and characterization, such as sputtering, heating, cooling and low energy electron diffraction. A fast entry lock allows rapid sample exchange and separate chambers, connected to the main one, will allow preparation of samples during measurements in the main station.

7. Conclusion

We conclude by presenting in Fig. 6 a picture of the beam line assembled in Trieste. All the mechanical parts have been aligned and the fine tuning of the optical elements, using the light coming from the undulator, is in progress.

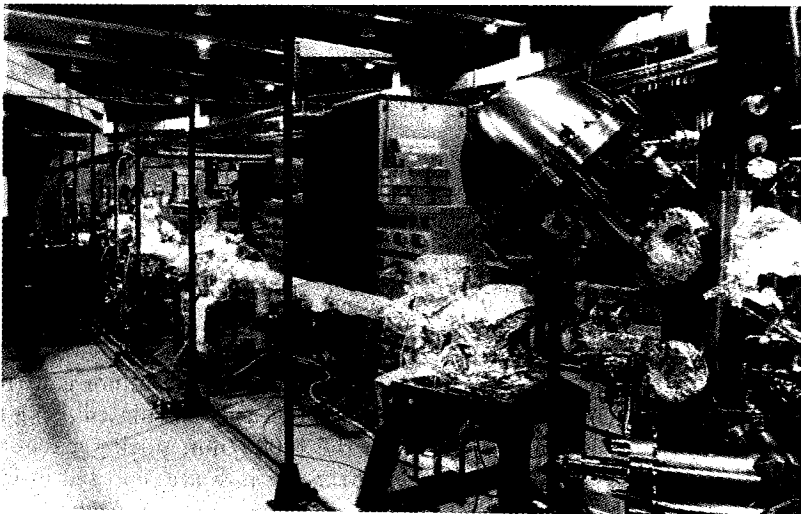


Fig. 6. View of the beam line.

Acknowledgments

We would like to thank the entire staff of "Sincrotrone Trieste" for the realization of the marvelous project "ELETTRA" and for having succeeded in such a very short time. Particularly we would like to thank Prof. C. Rubbia, Dr. G. Viani, Prof. M. Puglisi, Prof. A. Wrulich, Prof. R. Rosei and Prof G. Margaritondo for the incredible energy they put in making reality the fantastic dream "ELETTRA". Finally we would like to thank the company ISA ITALIA-JOBIN YVON for the excellent mechanical and optical work done in constructing the beam line. The work has been financed jointly from the Italian National Research Council and from the "Sincrotrone Trieste".

References

- [1] P. Kirkpatrick, A.V. Bacz, *J. Opt. Soc. Am.* **38**, 776 (1948).
- [2] J.C. Underwood, A.C. Thomson, J. Wu, R.D. Giaque, *Nucl. Instrum. Methods Phys. Res. A* **266**, 296 (1988).
- [3] C.T. Chen, *Nucl. Instrum. Methods Phys. Res. A* **256**, 595 (1987).
- [4] Conceptual Design for ELETTRA, Sincrotrone Trieste, Trieste 1989.
- [5] C.T. Chen, E.W. Plummer, M.R. Howells, *Nucl. Instrum. Methods Phys. Res. A* **222**, 103 (1984).
- [6] A.K. Freund, F. de Bergevin, G. Marot, C. Rickel, J. Susini, L. Zhang, E. Ziegler, *Opt. Eng.* **29**, 928 (1990).
- [7] C. Quaresima, *Calcolo della larghezza di banda della linea HERP*, ISM Internal report 31, Istituto di Struttura della Materia C.N.R., Frascati 1990.